J Comput Neurosci (2010) 28:77–89
DOI 10.1007/s10827-009-0188-9

A diffusion-activation model of CaMKII translocation waves in dendrites

Berton A. Earnshaw · Paul C. Bressloff

Received: 21 May 2009 / Revised: 6 August 2009 / Accepted: 16 September 2009 / Published online: 5 November 2009

Abstract Ca2+-calmodulin-dependent protein kinase II (CaMKII) is a key regulator of glutamatergic synapses and plays an essential role in many forms of synaptic plasticity. It has recently been observed that stimulating dendrites locally with a single glutamate/glycine puff induces a local translocation of CaMKII into spines that subsequently spreads in a wave-like manner towards the distal dendritic arbor. Here we present a mathematical model of the diffusion, activation and translocation of dendritic CaMKII. We show how the nonlinear dynamics of CaMKII diffusion-activation generates a propagating translocation wave, provided that the rate of activation is sufficiently fast. We also derive an explicit formula for the wave speed as a function of physiological parameters such as the diffusivity of CaMKII and the density of spines. Our model provides a quantitative framework for understanding the spread of CaMKII translocation and its possible role in heterosynaptic plasticity.

Action Editor: Wulfram Gerstner

B. A. Earnshaw · P. C. Bressloff (✉)
Department of Mathematics, University of Utah,
Salt Lake City, UT 84112-0090, USA
e-mail: bressloff@math.utah.edu, bressloff@maths.ox.ac.uk

P. C. Bressloff
Mathematical Institute, University of Oxford,
24–29 St. Giles', Oxford, OX1 3LB, UK

Keywords CaMKII · Reaction-diffusion equations · Traveling waves · Fisher's equation

1 Introduction

Perhaps no kinase has been more studied, especially in the context of synaptic plasticity, than Ca^{2+}–calmodulin-dependent protein kinase II (Ca MKII) (Hudmon and Schulman 2002; Lisman et al. 2002). CaMKII is abundant in the brain and particularly plentiful at postsynaptic densities (PSDs) where, bound to synaptic NMDA receptors (Gardoni et al. 1998; Leonard et al. 1999; Bayer et al. 2001), it is ideally situated to sense the spatiotemporal properties of Ca^{2+} entering the synapse as a result of plasticity-inducing protocols, and to subsequently phosphorylate substrates responsible for the expression of synaptic plasticity (Fukunaga et al. 1995; Mammen et al. 1997; Barria et al. 1997a; Derkach et al. 1999; Lee et al. 2000). In fact, CaMKII is essential for all known forms of NMDA receptor-dependent long-term potentiation (LTP) (Malinow et al. 1989; Fukunaga et al. 1993; Pettit et al. 1994; Lledo et al. 1995; Barria et al. 1997b; Otmakhov et al. 1997; Malenka and Bear 2004). What makes CaMKII such a potent player? While the binding of CaMKII to Ca^{2+}/CaM is necessary for its activation, once activated CaMKII can transition into a Ca^{2+}/CaM-independent, hyper-activated state via the autophosphorylation of neighboring enzymatic subunits (Hanson et al. 1994; Rich and Schulman 1998) comprising its unique holoenzyme architecture. In this autonomous state, CaMKII can continue to phosphorylate its substrates even after the plasticity-inducing Ca^{2+} signal has ended (Saitoh and Schwartz 1985;

Miller and Kenney 1986; Lou et al. 1986; Yang and Schulman 1999).

It has been known for some time that CaMKII translocates from the dendritic shaft into spines upon global stimulation of NMDA receptors (Strack et al. 1997; Shen and Meyer 1999; Shen et al. 2000; Bayer et al. 2006). In its inactive state the α isoform of CaMKII tends to be located in the cytosol whereas hetero-oligomers with β isoforms are weakly actin bound (Shen et al. 1998). Stimuli that trigger an increase in dendritic Ca^{2+} lead to the binding of Ca^{2+}/CaM to the CaMKII oligomer, which then allows the CaMKII to accumulate at postsynaptic sites through binding to NMDA receptors. If the calcium signal is relatively weak then this binding is rapidly reversible, whereas for stronger stimulation the synaptic accumulation of CaMKII can persist for several minutes due to autophosphorylation. Very recently it has been demonstrated that stimulating a region of dendrite with a 15 ms puff of 100 μM glutamate and 10 μM glycine not only induces the translocation of CaMKII into spines within the puffed region, but also initiates a wave of CaMKII translocation that spreads distally through the dendrite with an average speed of ~ 1 μm/s (Rose et al. 2009). The wave is preceded by a much faster Ca^{2+} spike mediated by L-type Ca^{2+} channels, and occurs in both pyramidal neurons and interneurons for both the α and β isoforms of CaMKII. The wave of CaMKII translocation is associated with an increase in AMPA receptor numbers at both stimulated and nonstimulated synapses (Rose et al. 2009), thus providing a possible molecular substrate for heterosynaptic plasticity.

The discovery of CaMKII translocation waves raises a number of important questions. For instance, how does the wave speed depend on the rates of diffusion, activation and translocation of CaMKII? Also, under what conditions does the wave fail to propagate? In order to address these questions, we propose a minimal mathematical model of CaMKII diffusion, activation and translocation into spines that captures the essential features of these waves. The model, which is an extension of the classical Fisher's equation for gene invasion (Fisher 1937; Kolmogorff et al. 1937), provides a quantitative framework for understanding the spread of CaMKII translocation and its possible role in heterosynaptic plasticity. Indeed, we show that the model supports waves of CaMKII translocation consistent with recent experimental findings (Rose et al. 2009), and provides a simple, explicit formula for the dependence of the wave speed on the model parameters. The model also exhibits wave propagation failure when the rate at which dendritic CaMKII translocates into spines is greater than the rate at which activated CaMKII activates primed CaMKII.

2 Model of CaMKII translocation waves

In this section we construct a minimal mathematical model of the diffusion, activation and translocation of CaMKII within a dendrite in order to test the following hypothesized mechanism for the generation and propagation of CaMKII translocation waves (Rose et al. 2009). Before local stimulation using a glutamate/glycine puff, the majority of CaMKII is in an inactive state and distributed uniformly throughout the dendrite. Upon stimulation, all CaMKII in the region of the puff (~ 30 μm of dendrite) is converted to an active state, probably the autonomous state of CaMKII (see Fig. 1(A)), and begins translocating into spines. Simultaneously, a Ca^{2+} spike is initiated and rapidly travels the length of the dendrite, causing CaMKII to bind Ca^{2+}/CaM along the way. In this primed or partially phosphorylated state, CaMKII does not yet translocate into spines. In the meantime, a portion of the activated CaMKII from the stimulated region diffuses into the region of primed CaMKII and the two types interact, with the result that primed CaMKII is activated. Some of these newly-activated holoenzymes translocate into spines while others diffuse into more distal regions of the dendrite containing primed CaMKII, and the wave proceeds in this fashion. In certain cases one also finds a second wave propagating proximally from the stimulated site to the soma (Rose et al. 2009). A schematic diagram illustrating the progression of a translocation wave along a dendrite following the rapid priming phase is shown in Fig. 1(B).

Our mathematical model takes the form of a system of reaction–diffusion equations for the concentrations of activated and primed CaMKII in the dendrite and spines. These equations incorporate three major components of the dynamics: *diffusion* of CaMKII along the dendrite, *activation* of primed CaMKII, and *translocation* of activated CaMKII from the dendrite to spines. For simplicity, we consider a uniform one-dimensional, nonbranching dendritic cable as shown in Fig. 1(A). We assume that a region of width 30 μm is stimulated with a glutamate/glycine puff at time $t = 0$. We take the center of the stimulated region to be at $x = 0$ and the distal end of the dendrite to be at $x = L = 150$ μm. The diffusion, activation and translocation of CaMKII

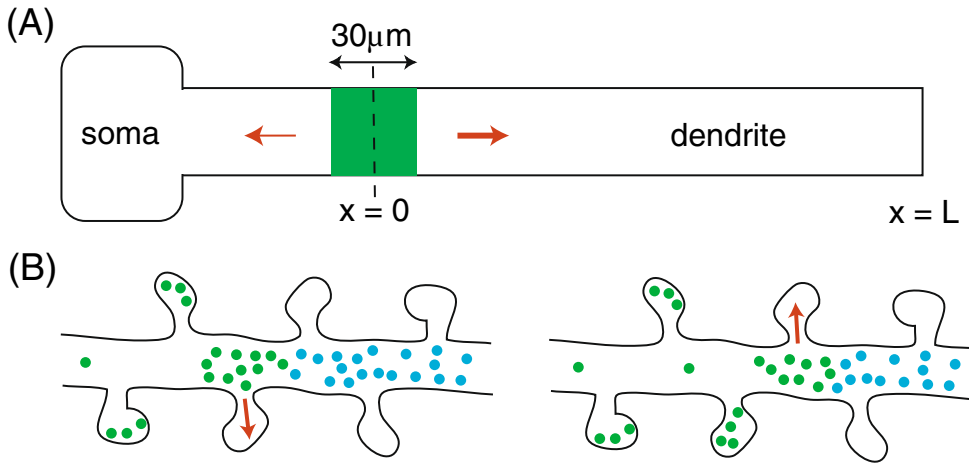

Fig. 1 Proposed mechanism of CaMKII translocation waves. (**A**) A glutamate/glycine puff activates CaMKII locally and initiates a Ca^{2+} spike (indicated by *red arrows*) that primes CaMKII in the remainder of the dendrite. (**B**) Activated CaMKII (*green dots*) both translocates into spines (*red arrows*) and diffuses into distal regions of the dendrite where it activates primed CaMKII (*blue dots*). The net effect is a wave of translocated CaMKII propagating along the dendrite

along the dendrite following stimulation is modeled according to the following system of equations:

$$\frac{\partial P}{\partial t} = D\frac{\partial^2 P}{\partial x^2} - k_0 A P \tag{2.1}$$

$$\frac{\partial A}{\partial t} = D\frac{\partial^2 P}{\partial x^2} + k_0 A P - hA \tag{2.2}$$

$$\frac{\partial S}{\partial t} = hA, \tag{2.3}$$

where D is the diffusivity of CaMKII within the cytosol. Here $P(x,t)$ and $A(x,t)$ denote the concentration of primed and activated CaMKII at time $t > 0$ and location x along the dendrite. $S(x,t)$ denotes the corresponding concentration of CaMKII in the population of spines at the same time and distance. For simplicity, we assume that all parameters are constant in space and time. The reaction term $k_0 AP$ represents the conversion of CaMKII from its primed to active state based on the irreversible first-order reaction scheme

$$A + P \to 2A$$

with mass action kinetics, where k_0 is the rate at which primed CaMKII is activated per unit concentration of activated CaMKII. The decay term hA represents the loss of activated CaMKII from the dendrite due to translocation into a uniform distribution of spines at a rate h. In our model we assume that translocation is irreversible over the time-scale of our simulations, which is reasonable given that activated CaMKII accumulation at synapses can persist for several minutes (Shen and Meyer 1999).

For simplicity, we model only the distal transport of CaMKII from the stimulated region by taking $0 \le x \le L$. Equations (2.1) and (2.2) are then supplemented by closed or reflecting boundary conditions at the ends $x = 0, L$. Hence, no CaMKII can escape from the ends. In reality activated CaMKII could also diffuse in the proximal direction and trigger a second proximal translocation wave. However, the choice of boundary condition has little effect on the results of our simulations. Taking the distal half of the stimulated region to be $0 \le x \le 15$ μm, we assume the following initial conditions: $P(x,0) = 0$ and $A(x,0) = C$ for $0 \le x \le 15$ μm, whereas $P(x,0) = P_0 \le C$ and $A(x,0) = 0$ for $x \ge 15$ μm, where C is the uniform resting concentration of CaMKII in the dendrite. Typical values of C range from 0.1 to 30 μM (Strack et al. 1997), covering two orders of magnitude. We also set $S(x,0) = 0$ everywhere. In other words, we assume that all the CaMKII is activated within the stimulated region at $t = 0$, but none has yet translocated into spines nor diffused into the nonstimulated region. We also neglect any delays associated with priming CaMKII along the dendrite. This is a reasonable approximation, since the Ca^{2+} spike travels much faster than the CaMKII translocation wave (Rose et al. 2009). Thus by the time a significant amount of activated CaMKII has diffused into

nonstimulated regions of the dendrite, any CaMKII encountered there will already be primed. The benefit of this assumption is that it eliminates the need to model the Ca^{2+} spike. However, a more detailed model that takes into account the initial transient associated with the priming phase could be constructed by coupling the reaction-diffusion equations with additional equations describing fast propagating dendritic spikes (Baer and Rinzel 1991; Coombes and Bressloff 2000).

It is convenient to introduce the normalized concentrations,

$$p = \frac{P}{P_0}, \quad a = \frac{A}{P_0}, \quad s = \frac{S}{P_0} \tag{2.4}$$

and re-express Eqs. (2.1–2.3) in terms of these variables according to

$$\frac{\partial p}{\partial t} = D\frac{\partial^2 p}{\partial x^2} - kap \tag{2.5}$$

$$\frac{\partial a}{\partial t} = D\frac{\partial^2 a}{\partial x^2} + kap - ha \tag{2.6}$$

$$\frac{\partial s}{\partial t} = ha, \tag{2.7}$$

where $k = k_0 P_0$ is the normalized activation rate. The initial condition for (normalized) primed CaMKII is then $p(x, 0) = 0$ when x is between 0 and 15 μm and $p(x, 0) = 1$ for $x > 15$ μm. The initial condition for (normalized) activated CaMKII is then obtained from the formula $a(x, 0) = a_0[1 - p(x, 0)]$, where $a_0 = C/P_0$. Note that in the absence of translocation into spines ($h = 0$) there is no loss of dendritic CaMKII, hence if we assume the initial condition $a_0 = 1$ then we have $a(x, t) + p(x, t) = 1$ for all x and t, and Eqs. (2.5–2.7) reduce to Fisher's equation for the invasion of a gene into a population (Fisher 1937; Kolmogorff et al. 1937):

$$\frac{\partial a}{\partial t} = D\frac{\partial^2 a}{\partial x^2} + ka(1 - a). \tag{2.8}$$

Interestingly, Eqs. (2.5) and (2.6) are identical in structure to a modification of Fisher's equation previously introduced to study the spatiotemporal spread of plagues such as the Black Death (Noble 1974).

3 Numerical results

The only parameters of the normalized model given by Eqs. (2.5–2.7) are the diffusivity D, the translocation rate h and the activation rate k. The translocation rate and diffusivity have been measured experimentally for both α and β isoforms (Shen et al. 1998; Shen and Meyer 1999). In the case of CaMKIIα, for example, $D \simeq 1$ μm^2/s and $h \simeq 0.01$/s. In this section we present numerical solutions of Eqs. (2.5–2.7) for both isoforms; the unknown activation rate k is then chosen so that the wave speed matches experimental values (Rose et al. 2009). All numerical simulations are produced with Matlab (MathWorks) using standard differential equation solvers.

In Fig. 2 we show the wave-like evolution of CaMKII for the α isoform. We plot concentration profiles at four successive snapshots in time, following stimulation of a local region of dendrite at an initial time $t = 0$ (Fig. 1(A)). We focus on the spread of CaMKII distally from the site of stimulation. It can be seen that a traveling pulse of activated CaMKII invades a region of primed CaMKII, activating the primed population along the way. As a consequence of this invasion and subsequent translocation into spines, the front of primed CaMKII retreats until all activated CaMKII has translocated into spines. We note that in this final state the relative increase of CaMKII in spines near the stimulated region is due to the initial condition (recall that at time $t = 0$, all CaMKII within the stimulated region is activated) and the fact that the translocation rate h is fast enough to allow spines in the stimulated region to "capture" a large portion of activated CaMKII before it diffuses away. The reduction at the end of the dendrite compensates for this increase in the stimulated region since the total amount of CaMKII must be conserved. Figure 3 further illustrates the different dynamical roles that primed and activated CaMKII play in producing the translocation wave. The composite wave consists of an advancing pulse of activated CaMKII superimposed upon a retreating front of primed CaMKII; both components propagate along the dendrite at the same speed c. The composite wave can be divided into three distinct spatial domains, each involving its own characteristic dynamics. Sufficiently distal from the initial site of activation, there is negligible activated CaMKII and an approximately uniform distribution of primed CaMKII. This corresponds to a quiescent region in which there is no net diffusive flux and no translocation into spines. On the other hand, sufficiently proximal to the initiation site, almost all of the primed CaMKII has been activated and the dynamics is dominated by translocation. Separating these two regions is the sharply rising part of the front where there is considerable overlap between the primed and activated CaMKII concentrations. Hence, in this interfacial region the dynamics is dominated by diffusion-activation that converts primed to activated CaMKII.

In Fig. 4 we show simulation results similar to Fig. 2, but this time using parameter values corresponding to

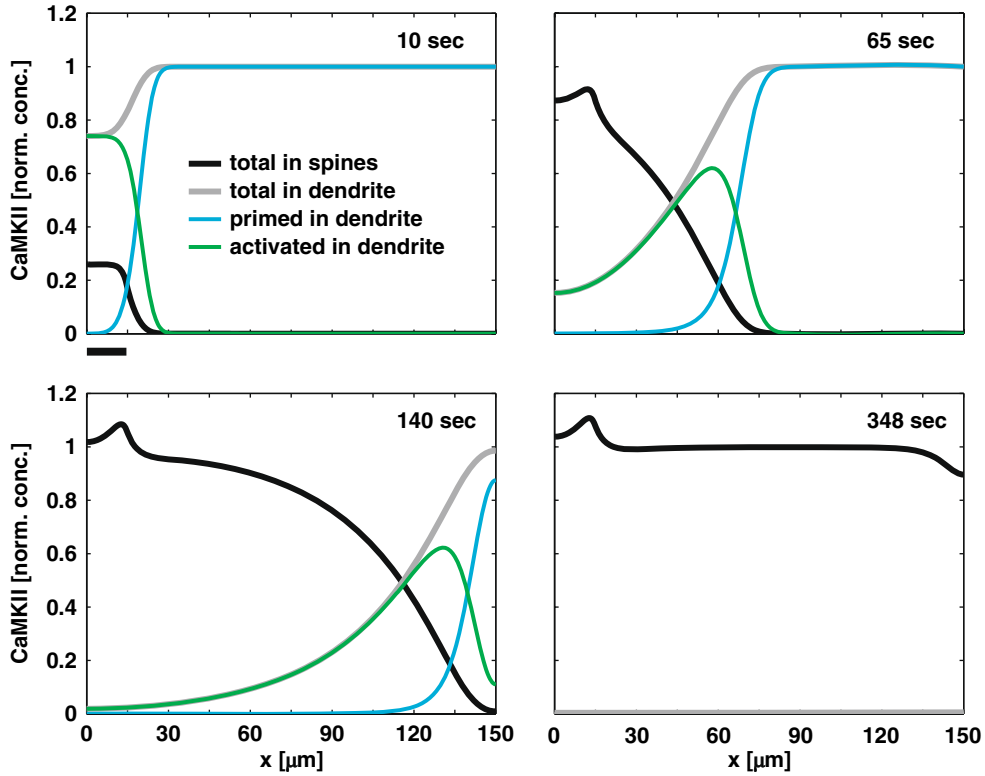

Fig. 2 Numerical simulation of a CaMKII translocation wave for the α isoform. Solutions of the diffusion-activation model (Eqs. (2.5–2.7)) are plotted for parameter values consistent with experimental data on CaMKIIα (Shen et al. 1998; Shen and Meyer 1999; Rose et al. 2009). The translocation rate $h = 0.03/s$, diffusivity $D = 1\ \mu m^2/s$ and the activation rate $k = 0.28/s$. At time $t = 0$ all of the CaMKII within the stimulated region (indicated by thick bar) is in the activated state, whereas all of the CaMKII within the nonstimulated region is in the primed state. Concentrations are normalized with respect to the initial concentration of primed CaMKII. Initially none of the activated CaMKII has translocated into spines. The resulting wave profiles for activated/primed CaMKII along the dendrite and translocated CaMKII within spines are shown at four successive snapshots in time. CaMKII is activated and translocated from dendrite to spine in a wave-like manner with a speed $c = 1\ \mu m/s$, until all the activated CaMKII is in spines

the β isoform of CaMKII rather than the α isoform. It can be seen that the CaMKIIβ wave (Fig. 4) propagates more slowly than the corresponding CaMKIIα wave (Fig. 2) for the same activation rate k. There are also differences in the wave profiles of the two isoforms. In particular, the CaMKIIβ activated and primed waves

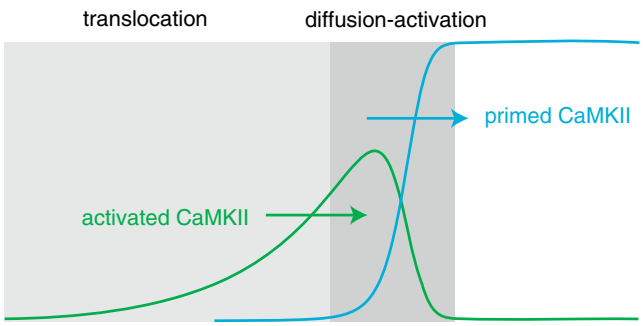

Fig. 3 Model wave profiles of activated and primed CaMKII concentrations along the dendrite. Arrows indicate direction of wave propagation. Composite wave consists of a pulse of activated CaMKII moving at the same speed as a front of primed CaMKII. The front forms an interface between a quiescent region containing a uniform concentration of primed CaMKII and a region dominated by translocation of activated CaMKII into spines. The dynamics in the interfacial region is dominated by diffusion-activation of primed CaMKII

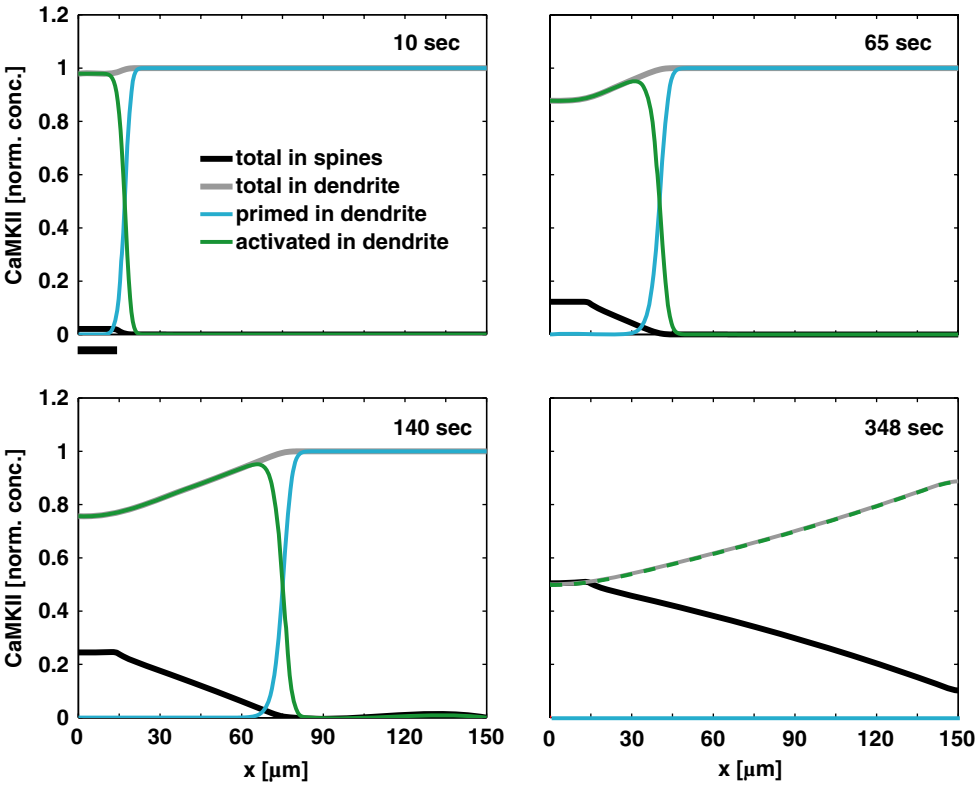

Fig. 4 Numerical simulation of a CaMKII translocation wave for the β isoform. Same as Fig. 2, except that the diffusivity D and translocation rate h are matched to experimental data for CaMKIIβ (Shen et al. 1998; Shen and Meyer 1999) ($D = 0.2\ \mu m^2/s$ and $h = 0.002/s$). CaMKIIβ is activated and translocated from dendrite to spine in a wave-like manner with a speed $c = 0.47\ \mu m/s$, which is slower than CaMKIIα for the same activation rate k but still in the observed range (Rose et al. 2009). There is still significant activated CaMKII within the dendritic shaft at the final time 348 s due to the slower translocation rate h of the β isoform

are steeper in the diffusion/activation region due to the smaller diffusivity of the β isoform, while the tail of the activated wave is less steep due to the smaller translocation rate of the β isoform.

In Fig. 5(A) we plot numerically determined values of the wave speed c for different values of k and show that these can be fitted exactly by the curve $c = 2\sqrt{D(k-h)}$. It turns out that this is the minimum possible speed of a traveling wave solution of our model for fixed D, h and k (see Section 4). The observation that the minimum wave speed is selected for the given initial conditions is related to the fact that our model equations are an extension of the classical Fisher's equation of population genetics (Fisher 1937; Kolmogorff et al. 1937). Indeed, we recover Fisher's equation when the rate of translocation h is zero (see

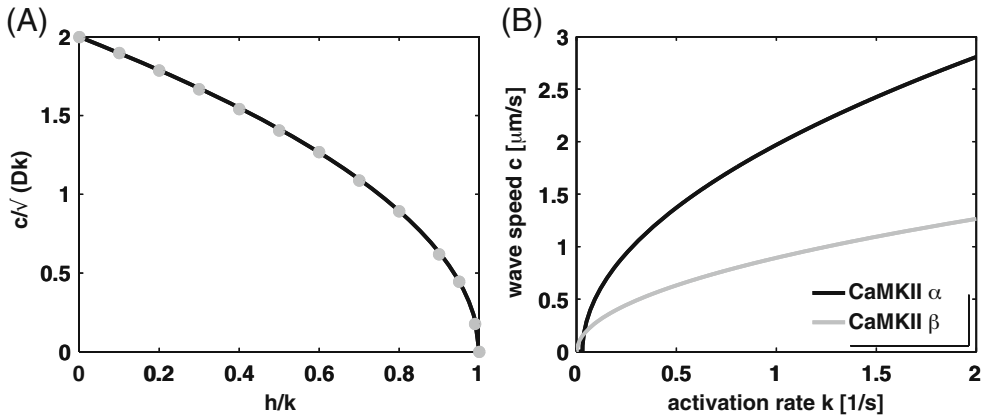

Fig. 5 Dependence of wave speed c on the activation rate k. (**A**) Plot of numerically determined values of the wavespeed c (in units of $\sqrt{Dk}$) against the ratio h/k (*gray circles*) obtained from simulations of the diffusion-activation model (Eqs. (2.5–2.7)) at different values of the activation rate k. Values of the diffusion coefficient D and translocation rate h used in the simulations are for the α isoform of CaMKII (see Fig. 2). The points are fitted by the black curve $c/\sqrt{Dk} = 2\sqrt{1 - h/k}$. (**B**) Plots of the analytically determined wave speed c as a function of the activation rate k for both α (*black curve*) and β (*gray curve*) isoforms of CaMKII

Eq. (2.8)). In this case the total amount of activated and primed CaMKII within the dendrite is conserved, yielding an advancing front of activated CaMKII superimposed upon a retreating front of primed CaMKII. The speed of the front is then $c = 2\sqrt{Dk}$. In Fig. 4(B), we plot the minimum wave speed c against the activation rate k for both the α and β isoforms of CaMKII. Our results suggest that CaMKIIα propagates more quickly than CaMKIIβ for the same activation rate. The curves in Fig. 5 provide a method for extracting the unknown activation rate k from experimental data on the translocation rate h, diffusivity D, and speed c of the translocation waves (Shen et al. 1998; Shen and Meyer 1999; Rose et al. 2009). Our model also predicts that if translocation is partially blocked by interfering with the binding of CaMKII to NMDA receptors at synaptic sites, the subsequent reduction in the translocation rate results in an increased wave speed.

One striking feature of Fig. 5(A) is that it predicts wave propagation failure when the translocation rate h is greater than the activation rate k, since in this case the predicted wave speed is purely imaginary and therefore nonphysical. This seems counterintuitive since one would expect that larger rates of translocation would promote the spread of translocation. However, if the translocation rate is greater than the activation rate, then activated CaMKII will tend to translocate into spines before activating primed CaMKII, thus preventing activated CaMKII from spreading through the dendritic shaft. Figure 6 shows a simulation of this phenomenon for the α isoform of CaMKII. Although at short times the CaMKII concentrations appear similar to those in Fig. 2, as time progresses we see that activated CaMKII is quickly translocated into spines, whence the translocation wave fails to propagate. The translocation rate can be written as $h = \rho h_0$, where ρ is the density of spines and h_0 is the translocation rate per spine. Similarly, the activation rate can be expressed as $k = k_0 P_0$ where P_0 is the initial concentration of primed CaMKII in the nonstimulated region of the dendrite and k_0 is the activation rate per unit concentration of activated CaMKII. Thus our model predicts that CaMKII translocation waves will fail to propagate when

$$\rho h_0 > k_0 P_0 \tag{3.1}$$

For example, this inequality predicts that dendrites with a high density of spines are less likely to exhibit translocation waves than those with a low spine density. It also predicts that dendrites with a larger initial concentration of primed CaMKII in the shaft are more likely to exhibit translocation waves than those with a smaller initial concentration. Since the initial concentration P_0 of primed CaMKII depends on both

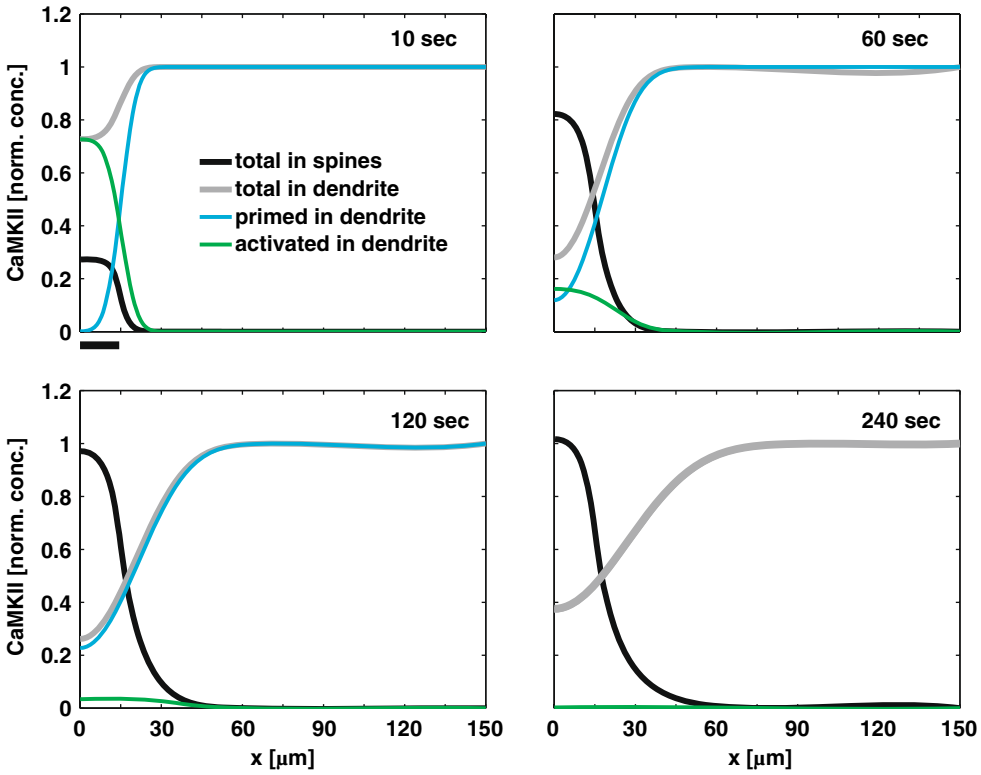

Fig. 6 Wave propagation failure when the translocation rate h is greater than the activation rate k. Same as Fig. 2, except the activation rate for CaMKII is taken to be $k = 0.028/s$, which is now smaller than the translocation rate of $h = 0.03/s$. Activated CaMKII is translocated into spines before it activates primed CaMKII, causing the translocation wave to fail

the initial concentration of inactive CaMKII within the dendrite and the effectiveness of the Ca^{2+} spike in both propagating along the dendrite and priming the inactive state, our model agrees with the experimental finding that translocation waves fail to propagate when L-type Ca^{2+} channels are blocked (Rose et al. 2009).

3.1 Decay of primed CaMKII

So far we have assumed that over the time-scale of our simulations any spontaneous decay of activated or primed CaMKII is negligible. In the case of activated CaMKII, this assumption is consistent with experimental observations regarding the persistence of phosphorylated CaMKII following the induction of LTP (Fukunaga et al. 1995; Barria et al. 1997b; Lisman et al. 2002) (but see Lee et al. 2009). However, it is less clear to what extent the primed state of CaMKII is stable. Therefore, it is important to determine how our results are modified if decay of primed CaMKII is included. Intuitively one would expect that our results regarding translocation waves would still approximately hold provided that the time constant for the decay of primed CaMKII is larger than the time-scale of our simulations. On the other hand, if the decay is sufficiently fast then wave propagation failure will occur, since there will not be a sufficient concentration of primed CaMKII remaining in distal regions of the dendrite by the time the wave of activated CaMKII arrives.

In order to verify the above, we numerically simulated a modified version of Eqs. (2.5–2.7) given by

$$\frac{\partial p}{\partial t} = D\frac{\partial^2 p}{\partial x^2} - kap - \varepsilon p \tag{3.2}$$

$$\frac{\partial a}{\partial t} = D\frac{\partial^2 a}{\partial x^2} + kap - ha \tag{3.3}$$

$$\frac{\partial s}{\partial t} = ha, \tag{3.4}$$

where ϵ is the rate of decay of primed CaMKII back to its native state. The results are shown in Figs. 7 and 8. It can be seen from Fig. 7 that over the time course of several hundred seconds, an approximate translocation wave occurs when $\varepsilon = 0.001$/s. It is important to note that from a mathematical perspective Eqs. (3.2–3.4) do not support an exact traveling wave solution, that is, a solution with a constant wave speed and an invariant wave profile (away from boundaries). Indeed, the amplitude of the wave decreases with time, reflecting the slow decay of primed CaMKII. In the case of faster decay, wave propagation failure occurs over the time-scale of the simulations, as shown in Fig. 8.

Given that translocation waves are observed to propagate for several minutes (Rose et al. 2009), and assum-

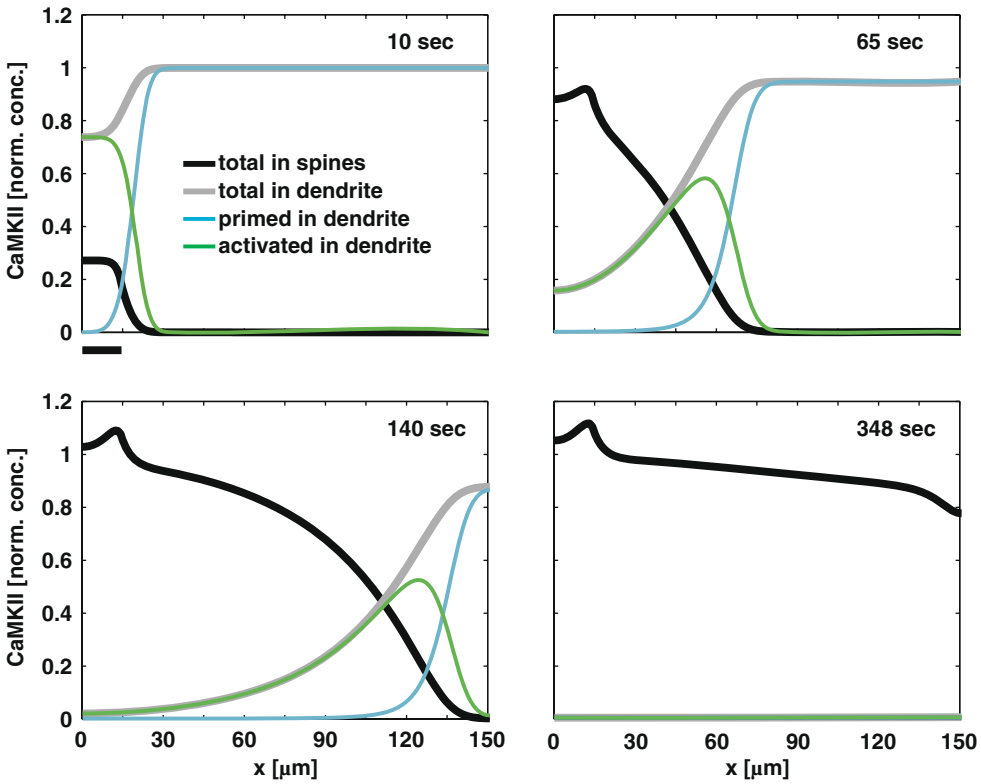

Fig. 7 Numerical simulation of an approximate CaMKII translocation wave when primed CaMKII decays back to its native state at a relatively slow rate of $\epsilon = 0.001$/s. Other parameter values as in Fig. 2

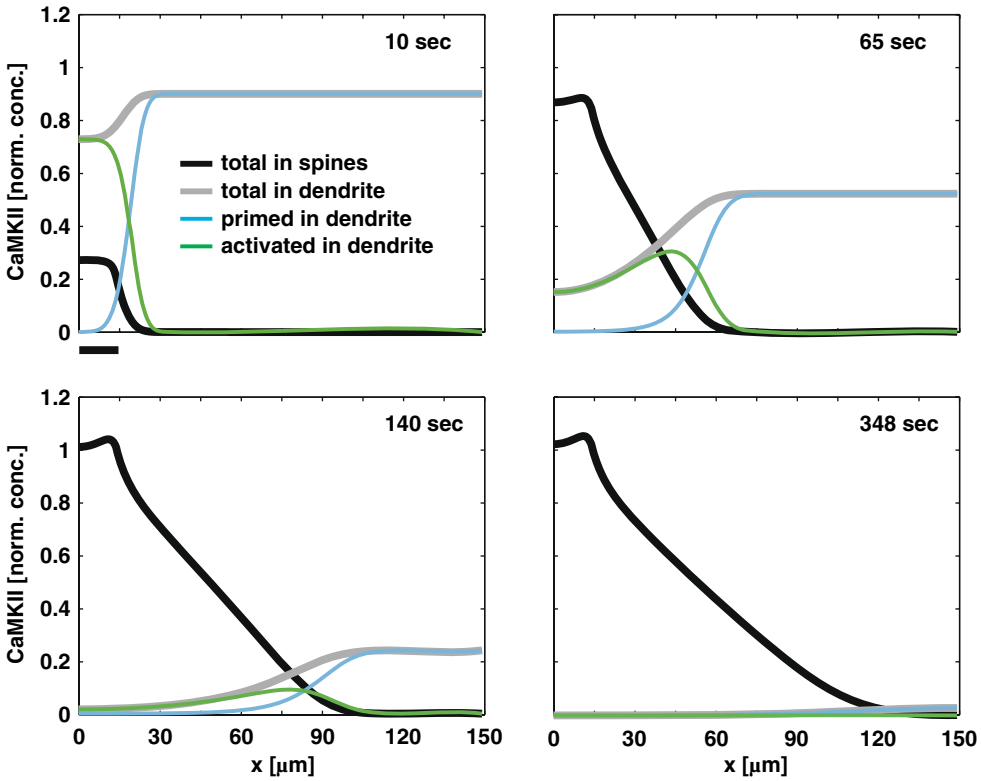

Fig. 8 Numerical simulation showing wave propagation failure when primed CaMKII decays quickly at a rate $\epsilon = 0.01/s$. Other parameter values as in Fig. 2

ing that the hypothesized mechanism for translocation waves is correct, it would then follow that CaMKII can exist in a relatively stable primed (but not fully activated) state. This remains to be tested experimentally. It would also be interesting to measure the predicted changes in the rate or amplitude of the translocation wave as it propagates due to the effects of decay of primed CaMKII.

4 Calculation of minimal wave speed

In order to derive a formula for the speed c of CaMKII translocation waves (in the absence of decay), we assume a traveling wave solution of the form $p = p(x - ct)$ and $a = a(x - ct)$. Introducing the traveling wave coordinate $z = x - ct$, we find that Eqs. (2.5) and (2.6) are transformed to

$$-c\frac{dp}{dz} = D\frac{d^2p}{dz^2} - kap \tag{4.1}$$

$$-c\frac{da}{dz} = D\frac{d^2a}{dz^2} + kap - ha \tag{4.2}$$

This is a system of two second-order ordinary differential equations in the variable z. A global view of the nature of traveling wave solutions can be obtained by identifying Eqs. (4.1) and (4.2) with the equation of motion of a classical particle in two spatial dimensions undergoing damping due to "friction" and subject to an "external force". Thus we identify a and p with the "spatial" coordinates of the particle, z with the corresponding "time" coordinate, and the speed c as a "friction coefficient". If we ignore boundary effects by taking $-\infty < z < \infty$, then we can view a traveling wave solution as a particle trajectory that connects the point $(p, a) = (p^*, 0)$ at $z = -\infty$ (with $p^* < 1$) to the point $(p, a) = (1, 0)$ at $z = \infty$. A restriction on the allowed values of c can now be obtained by investigating how the point $(1, 0)$ is approached in the large-z limit. Linearizing Eqs. (4.1) and (4.2) about the point $(p, a) = (1, 0)$ we obtain a pair of second-order linear equations, which have solutions of the form $(p, a) = \mathbf{V}e^{-\lambda z}$ where λ and $\mathbf{V}$ satisfy the matrix equation

$$c\lambda\mathbf{V} = \begin{pmatrix} D\lambda^2 & -k \\ 0 & D\lambda^2 + k - h \end{pmatrix}\mathbf{V} \tag{4.3}$$

Solving for the eigenvalue λ leads to the four solutions

$$\lambda = 0, \quad \frac{c}{D}, \quad \frac{c \pm \sqrt{c^2 - 4D(k-h)}}{2D} \tag{4.4}$$

and these, along with their corresponding eigenvectors $\mathbf{V}$, determine the shape of the wave as it approaches the point $(1, 0)$. Note that the last two eigenvalues

have a nonzero imaginary part when $c^2 < 4D(k-h)$, implying that as z becomes large the wave oscillates about the point $(1,0)$. This cannot be allowed since it would imply that the normalized activated CaMKII concentration a takes on negative values (inspection of the corresponding eigenvectors show that their components in the a-direction are nonzero and so a would indeed oscillate). Therefore, we must have

$$c \geq c_{\min} = 2\sqrt{D(k-h)} \tag{4.5}$$

The fact that the observed wave speed in our simulations takes this minimum value can be understood by considering the more general theory of so-called pulled-fronts, which has been applied to various generalizations of Fisher's equation, see the review van Saarloos (2003) and references therein.

5 Discussion

We have shown that a minimal mathematical model of the dendritic diffusion, activation and translocation of CaMKII into spines reproduces the waves of distally-propagating CaMKII translocation that were observed recently in experiments (Rose et al. 2009). The model is a mathematical implementation of a hypothetical mechanism suggested by the experiments (Rose et al. 2009), and the fact that the model exhibits translocation waves provides support for this mechanism. In addition, from the model we derived an exact and simple formula relating the speed c of the translocation wave to the diffusivity D, activation rate k and translocation rate h of CaMKII, see Eq. (4.5). This formula is a prediction of the model and provides a way to test its validity. It also allows for the estimation of the experimentally undetermined activation rate k. In addition, we showed that translocation fails to propagate when the translocation rate h is larger than the activation rate k. This observation both confirms experimental results, e.g. CaMKII priming is necessary for wave propagation (Rose et al. 2009), and offers additional predictions, e.g. dendrites with dense spine populations are less likely to exhibit CaMKII translocation waves than those with sparse spine populations.

Heterosynaptic plasticity. The possibility of initiating waves of CaMKII translocation has important implications for heterosynaptic plasticity. Indeed, it was observed that the AMPA receptor subunit GluR1 coaccumulates with CaMKII in spines following such waves (Rose et al. 2009), and the up-regulation of AMPA receptor numbers in synapses is a well-established mechanism for the expression of long-term potentiation (LTP) (Malenka and Bear 2004). While heterosynaptic LTP has been observed in many different preparations (Bi and Poo 2001), producing effects at lengths greater than ~ 10 μm often requires that a spatially-localized cluster of synapses be stimulated simultaneously (Rose et al. 2009; Engert and Bonhoeffer 1997). Moreover, recent studies find that inducing LTP at a single synapse activates CaMKII within the spine containing the synapse but neither induces LTP at nearby synapses nor raises CaMKII content in nearby spines (Zhang et al. 2008; Lee et al. 2009). Taken together, these findings suggest the existence of a threshold that the concentration of activated CaMKII in the dendritic shaft must obtain before a translocation wave can be initiated (see below). Note, however, that the induction of LTP at a single synapse has been shown to lower the induction threshold of LTP at synapses within $\sim$ 10 μm (Harvey and Svoboda 2007). Thus there are likely many mechanisms mediating heterosynaptic effects at different length scales, with CaMKII translocation waves mediating one of the longest. Consequently, CaMKII translocation waves likely play an important role in the "tagging" of neighboring synapses for subsequent heterosynaptic regulation (Frey and Morris 1997; Reymann and Frey 2007).

Threshold for wave initiation. As discussed in the previous paragraph, we expect CaMKII wave propagation failure to occur if the initial stimulus is weak or confined to too narrow a region of dendrite. This is likely due to the inability of the weak stimulus to either initiate a Ca^{2+} spike or produce enough activated CaMKII to successfully encounter and react with primed CaMKII. Recall that we do not model the Ca^{2+} spike explicitly since it appears to be much faster than the CaMKII translocation wave (Rose et al. 2009). However, the effect of the Ca^{2+} spike is included in the model indirectly via the initial concentration P_0 of primed CaMKII. If a weak stimulus initiates a slow Ca^{2+} spike or no spike at all, then $P_0 \approx 0$ for significant portions of the dendrite. In these regions the activation rate $k = k_0 P_0 \approx 0$ and so will likely be smaller than the translocation rate h, leading to wave propagation failure in our model. Interestingly, the speed of a Ca^{2+} spike is expected to increase with increasing spine density (Baer and Rinzel 1991; Coombes and Bressloff 2000), while according to our model the CaMKII translocation wave speed is expected to decrease, hence for some spine density levels it may be necessary to model both waves in order to determine whether or not the translocation wave will propagate. The model does not, however, exhibit wave propagation failure when there is only a small initial amount of activated CaMKII in the stimu-

lated region. This is because the model tracks only the concentration of CaMKII throughout the dendrite and not the location of individual CaMKII holoenzymes. While such an approach simplifies the model, allowing one to make explicit the manner in which CaMKII translocation waves are propagated, it does neglect stochastic effects due to fluctuations in the number and location of CaMKII holoenzymes that may result in wave propagation failure. We hope to study the effect of such fluctuations on translocation wave initiation in future work.

Heterogeneities. A major simplifying assumption of the model is that the dendrite is uniform and non-branching, with rates of diffusion, activation and translocation of CaMKII that are the same throughout the dendrite. These assumptions simplify the mathematical analysis and allow for the exact calculation of the speed of the predicted translocation wave. Although it would be possible to extend the model to take into account various forms of heterogeneities along the dendrite, the basic mechanisms of CaMKII translocation wave initiation, propagation and failure would still apply. Indeed, our analysis of the wave speed would still hold provided that the spatial variation in physiological parameters was negligible over the length-scale of the interfacial region of the front (see Fig. 3). Another source of heterogeneity arises from the discrete nature of dendritic spines. In our model we assume that rate of translocation is spatially uniform along the dendrite. However, recall that h depends on the density of spines ρ according to $h = \rho h_0$, with h_0 the translocation rate per spine. Hence, we are effectively representing the population of spines as a uniform density rather than as a set of discrete objects. This should not effect our results significantly since a typical spine density ρ is $\sim 1\ \mu\text{m}^{-1}$ (Harms and Craig 2005), while typical values for diffusion coefficient D and the translocation rate h of CaMKIIα are respectively $\sim 1\ \mu\text{m}^2/\text{s}$ (Shen et al. 1998) and $\sim 0.01/\text{s}$ (Shen and Meyer 1999), implying that on the time scale of translocation, the effective length scale of diffusion is $\sim 10\ \mu\text{m}$; i.e., we expect that activated CaMKIIα will on average diffuse 10 μm before entering a spine, passing by an average of 10 spines on the way (a similar conclusion can be made for CaMKIIβ). Nevertheless, it would be possible to take into account the effects of discrete spines in our model by using homogenization theory (Meunier and d'Incamps 2008; Bressloff 2009). Finally, note that although we focus on CaMKII translocation waves in spiny dendrites, such waves have also been observed in aspiny interneurons (Rose et al. 2009). If we wish to model these waves then we need only reinterpret the parameter h in Eq. (2.3) as the translocation rate of dendritic CaMKII into synapses, not spines, and reinterpret the variable S as the corresponding synaptic CaMKII concentration.

Diffusion and trapping in dendritic spines. The model presented in this paper is one of a class of mathematical models concerned with understanding the interplay between diffusion and other modes of molecular transport in dendrites on one hand, and the trapping of molecules within the spine compartment on the other. Examples of such diffusion-trapping models include those concerned with AMPA receptor trafficking and its role in synaptic plasticity (Newpher and Ehlers 2008; Holcman and Triller 2006; Earnshaw and Bressloff 2006, 2008). Many diffusion-trapping models predict that the combination of dendritic diffusion and spine trapping results in the subdiffusive transport of proteins along the length of the dendrite (Bressloff and Earnshaw 2007; Santamaria et al. 2006; Dagdug et al. 2007). In contrast, in the present model the combination of diffusion and trapping via translocation into spines is not the dominant transport mechanism. Rather, the combination of diffusion and activation of primed CaMKII by activated CaMKII results in the ballistic motion of the translocation wave, and spine trapping only modulates the speed of the wave. Similar to the propagation of an action potential along an axon, the regenerative effects of CaMKII activation overcome the dissipative effects of diffusion and trapping which would otherwise quench such transport.

Acknowledgement This work was supported by the National Science Foundation (DMS 0813677 and RTG 0354259).

References

Baer, S. M., & Rinzel, J. (1991). Propagation of dendritic spikes mediated by excitable spines: A continuum theory. *Journal of Neurophysiology, 65*, 874–890.

Barria, A., Derkach, V., & Soderling, T. (1997a). Identification of the Ca2+/calmodulin-dependent protein kinase II regulatory phosphorylation site in the α-amino-3-hydroxyl-5-methyl-4-isoxazole-proprionic acid glutamate receptor. *Journal of Biological Chemistry, 272*, 32727–32730.

Barria, A., Muller, D., Derkach, V., Griffith, L. C., & Soderling, T. R. (1997b). Regulatory phosphorylation of AMPA-type glutamate receptors by CaMKII during long-term potentiation. *Science, 276*, 2042–2045.

Bayer, K. U., De Koninck, P., Leonard, A. S., Hell, J. W., & Schulman, H. (2001). Interaction with the NMDA receptor locks CaMKII in an active conformation. *Nature, 411*, 801–805.

Bayer, K. U., et al. (2006). Transition from reversible to persistent binding of CaMKII to postsynaptic sites and NR2B. *Journal of Neuroscience, 26*, 1164–1174.

Bi, G.-Q., & Poo, M.-M. (2001). Synaptic modification by correlated activity: Hebb's postulate revisited. *Annual Review of Neuroscience, 24*, 139–166.

Bressloff, P. C. (2009). Cable theory of protein receptor trafficking in dendritic trees. *Physics Review E, 79*, 041904.

Bressloff, P. C., & Earnshaw, B. A. (2007). Diffusion-trapping model of receptor trafficking in dendrites. *Physics Review E, 75*, 041915.

Coombes, S., & Bressloff, P. C. (2000). Solitary waves in a model of dendritic cable with active spines. *SIAM Journal of Applied Mathematics, 61*, 432–453.

Dagdug, L., Berezhkovskii, A. M., Makhnovskii, Y. A., & Zitserman, V. Y. (2007). Transient diffusion in a tube with dead ends. *Journal of Chemical Physics, 127*, 224712.

Derkach, V., Barria, A., & Soderling, T. R. (1999). Ca^{2+}/calmodulin-kinase II enhances channel conductance of α-amino-3-hydroxyl-5-methyl-4-isoxazoleproprionate type glutamate receptors. *Proceedings of the National Academy of Sciences of the United States of America, 96*, 3269–3274.

Earnshaw, B. A., & Bressloff, P. C. (2006). Biophysical model of AMPA receptor trafficking and its regulation during long-term potentiation/long-term depression. *Journal of Neuroscience, 26*, 12362–12373.

Earnshaw, B. A., & Bressloff, P. C. (2008). Modeling the role of lateral membrane diffusion in AMPA receptor trafficking along a spiny dendrite. *Journal of Computational Neuroscience, 25*, 366–389.

Engert, F., & Bonhoeffer, T. (1997). Synapse specificity of long-term potentiation breaks down at short distances. *Nature, 388*, 279–284.

Fukunaga, K., Stoppini, L., Miyamoto, E., & Muller, D. (1993). Long-term potentiation is associated with an increased activity of Ca^{2+}/calmodulin-dependent protein kinase II. *Journal of Biological Chemistry ,268*, 7863–7867.

Fukunaga, K., Muller, D., & Miyamoto, E. (1995). Increased phosphorylation of Ca^{2+}/calmodulin-dependent protein kinase II and its endogenous substrates in the induction of long-term potentiation. *Journal of Biological Chemistry, 270*, 6119–6124.

Gardoni, F., et al. (1998). Calcium/calmodulin-dependent protein kinase II is associated with NR2A/B subunits of NMDA receptor in postsynaptic densities. *Journal of Neurochemistry, 71*, 1733–1741.

Hanson, P. I., Meyer, T., Stryer, L., & Schulman, H. (1994). Dual role of calmodulin in autophosphorylation of multifunctional CaM Kinase may underlie decoding of calcium signal. *Neuron, 12*, 943–956.

Harms, K. J., & Craig, A. M. (2005). Synapse composition and organization following chronic activity blockade in cultured hippocampal neurons. *Journal of Comparative Neurology, 490*, 72–84.

Harvey, C. D., & Svoboda, K. (2007). Locally dynamic synaptic learning rules in pyramidal neuron dendrites. *Nature, 450*, 1195–1202.

Holcman, D., & Triller, A. (2006). Modeling synaptic dynamics driven by receptor lateral diffusion. *Biophysical Journal, 91*, 2405–2415.

Hudmon, A., & Schulman, H. (2002). Neuronal Ca2+/calmodulin-dependent protein kinase II: The role of structure and autoregulation in cellular function. *Annual Review of Biochemistry, 71*, 473–510.

Fisher, R. A. (1937). The wave of advance of advantageous genes. *Annals of Eugenics, 7*, 353–369.

Frey, U., & Morris, R. (1997). Synaptic tagging and long-term potentiation. *Nature, 385*, 533–536.

Kolmogorff, A., Petrovsky, I., & Piscounoff, N. (1937). Étude de l'équation de la diffusion avec croissance de la quantité de matière et son application à un problème biologique. *Bulletin of Mathematics, 1*, 1–25 (Moscow University).

Lee, H.-K., Barbarosie, M., Kameyama, K., Bear, M. F., & Huganir, R. L. (2000). Regulation of distinct AMPA receptor phosphorylation sites during bidirectional synaptic plasticity. *Nature, 405*, 955–959.

Lee, S.-J. R., Escobedo-Lozoya, Y., Szatmari, E. M., & Yasuda, R. (2009). Activation of CaMKII in single dendritic spines during long-term potentiation. *Nature, 458*, 299–304.

Leonard, A. S., Lim, I. A., Hemsworth, D. E., Horne, M. C., & Hell, J. W. (1999). Calcium/calmodulin-dependent protein kinase II is associated with the N-methyl-D-aspartate receptor. *Proceedings of the National Academy of Sciences of the United States of America, 96*, 3239–3244.

Lisman, J., Schulman, H., & Cline, H. (2002). The molecular basis of CaMKII function in synaptic and behavioural memory. *Nature Reviews. Neuroscience, 3*, 175–190.

Lledo, P. M., et al. (1995). Calcium/calmodulin-dependent kinase II and long-term potentiation enhance synaptic transmission by the same mechanism. *Proceedings of the National Academy of Sciences of the United States of America, 92*, 11175–11179.

Lou, L. L., Lloyd, S. J., & Schulman, H. (1986). Activation of the multifunctional Ca^{2+}/calmodulin-dependent protein kinase by autophosphorylation: ATP modulates production of an autonomous enzyme. *Proceedings of the National Academy of Sciences of the United States of America, 83*, 9497–9501.

Malenka, R. C., & Bear, M. F. (2004). LTP and LTD: An embarrassment of riches. *Neuron, 44*, 5–21.

Malinow, R., Schulman, H., & Tsien, R. W. (1989). Inhibition of postsynaptic PKC or CaMKII blocks induction but not expression of LTP. *Science, 245*, 862–866.

Mammen, A. L., Kameyama, K., Roche, K. W., & Huganir, R. L. (1997). Phosphorylation of the α-amino-3-hydroxyl-5-methyl-isoxazole-4-proprionic acid receptor GluR1 subunit by calcium/calmodulin-dependent protein kinase II. *Journal of Biological Chemistry, 272*, 32528–32533.

Meunier, C., & d'Incamps, B. L. (2008). Extending cable theory to heterogeneous dendrites. *Neural Computation, 20*, 1732–1775.

Miller, S. G., & Kenney, M. B. (1986). Regulation of brain type II Ca^{2+}/calmodulin-dependent protein kinase by autophosphorylation: A Ca^{2+}-triggered molecular switch. *Cell, 44*, 861–870.

Newpher, T. M., & Ehlers, M. D. (2008). Glutamate receptor dynamics in dendritic microdomains. *Neuron, 58*, 472–497.

Noble, J. V. (1974). Geographic and temporal development of plagues. *Nature, 250*, 726–729.

Otmakhov, N., Griffith, L. C., & Lisman, J. E. (1997). Postsynaptic inhibitors of calcium/calmodulin-dependent protein kinase type II block induction but not maintenance of pairing-induced long-term potentiation. *Journal of Neuroscience, 17*, 5357–5365.

Pettit, D. L., Perlman, S., & Malinow, R. (1994). Potentiated transmission and prevention of further LTP by increased CaMKII activity in postsynaptic hippocampal slice neurons. *Science, 266*, 1881–1885.

Reymann, K., & Frey, J. (2007). The late maintenance of hippocampal LTP: Requirements, phases, synaptic tagging, late associativity and implications. *Neuropharmacology, 52*, 24–40.

Rich, R. C., & Schulman, H. (1998). Substrate-directed function of calmodulin in autophosphorylation of Ca2+/calmodulin-

dependent protein kinase II. *Journal of Biological Chemistry, 273*, 28424–28429.

Rose, J., Jin, S.-X., & Craig, A. M. (2009). Heterosynaptic molecular dynamics: Locally induced propagating synaptic accumulation of CaM Kinase II. *Neuron, 61*, 351–358.

Saitoh, T., & Schwartz, J. H. (1985). Phosphorylation-dependent subcellular translocation of a Ca^{2+}/calmodulin-dependent protein kinase produces an autonomous enzyme in Aplysia neurons. *Journal of Cell Biology, 100*, 835–842.

Santamaria, F., Wils, S., De Schutter, E., & Augustine, G. J. (2006). Anomalous diffusion in Purkinje cell dendrites caused by spines. *Neuron, 52*, 635–648.

Shen, K, & Meyer, T. (1999). Dynamic control of CaMKII translocation and localization in hippocampal neurons by NMDA receptor simulation. *Science, 284*, 162–166.

Shen, K., Tereul, M. N., Subramanian, K., & Meyer, T. (1998). CaMKIIβ functions as an F-actin targeting module that localizes CaMKIIα/β heterooligomers to dendritic spines. *Neuron, 21*, 593–606.

Shen, K., Teruel, M. N., Connor, J. H., Shenolikar, S., & Meyer, T. (2000). Molecular memory by reversible translocation of calcium/calmodulin-dependent protein kinase II. *Nature Neuroscience, 3*, 881–886.

Strack, S., Choi, S., Lovinger, D. M., & Colbran, R. J. (1997). Translocation of autophosphorylated calcium/calmodulin-dependent protein kinase II to the postsynaptic density. *Journal of Biological Chemistry, 272*, 13467–13470.

van Saarloos, W. (2003). Front propagation into unstable states. *Physics Reports, 386*, 29–222.

Yang, E., & Schulman, H. (1999). Structural examination of autoregulation of multifunctional calcium/calmodulin-dependent protein kinase II. *Journal of Biological Chemistry, 274*, 26199–26208.

Zhang, Y.-P., Holbro, N., & Oertner, T. G. (2008). Optical induction of plasticity at single synapses reveals input-specific accumulation of αCaMKII. *Proceedings of the National Academy of Sciences of the United States of America, 105*, 12039–12044.